

Demonstration of an Optimized Large-scale Optogenetic Cortical Interface for Non-human Primates*

Devon J. Griggs, Julien Bloch, Shawn Fisher, William K. S. Ojemann, Kali M. Coubrough, Karam Khateeb, Marcus Chu, and Azadeh Yazdan-Shahmorad, *Member, IEEE*

Abstract— Optogenetics is a powerful neuroscientific tool which allows neurons to be modulated by optical stimulation. Despite widespread optogenetic experimentation in small animal models, optogenetics in non-human primates (NHPs) remains a niche field, particularly at the large scales necessary for multi-regional neural research. We previously published a large-scale, chronic optogenetic cortical interface for NHPs which was successful but came with a number of limitations. In this work, we present an optimized interface which improves upon the stability and scale of our previous interface while using more easily replicable methods to increase our system's availability to the scientific community. Specifically, we (1) demonstrate the long-term (~3 months) optical access to the brain achievable using a commercially-available transparent artificial dura with embedded electrodes, (2) showcase large-scale optogenetic expression achievable with simplified (magnetic resonance-free) surgical techniques, and (3) effectively modulated the expressing areas at large scales (~1 cm²) by light emitting diode (LED) arrays assembled in-house.

I. INTRODUCTION

Optogenetics, a technique by which cells can be genetically modified to be sensitive to light, has proven itself as a powerful tool for neuroscience [1]. A small but growing subset of the scientific community has used optogenetics in non-human primate (NHP) neuroscience research [2]–[5], and our lab has pioneered large-scale cortical optogenetics in NHPs with simultaneous electrocorticography [6]–[10]. To our knowledge, our previous work is the largest and longest-lasting demonstration of optogenetics in NHPs [7], [8].

While successful, our previous methods had a few key limitations: 1) The optical window provided only about four weeks of optical access clear enough for optogenetic experimentation before accelerated tissue growth obscured the brain and tissue resection was required [7]–[9]. This contrasts starkly with 3-9 months of optical access achievable with classic, electrode-free optical windows [8], [11]–[13]. 2) Our optogenetic infusion technique required live magnetic resonance imaging (MRI) guidance of contrast agent co-infused with viral vector during NHP neural surgery. This technique is helpful for monitoring the infusion of the virus but unfortunately the capability is not widely available to the scientific community [7]–[9]. 3) Our experimental setup was limited to 2-3 sites of simultaneous light stimulation using fiber optics [7], [8] and lacked the ability to simultaneously

control the activity of a broad cortical area needed for large-scale experiments.

In this work, we increase the scientific community's accessibility to large-scale cortical optogenetics in NHPs by developing an interface which solves the aforementioned limitations.

II. METHODS

A. Animal

We performed all surgical and experimental procedures on one healthy adult rhesus macaque (*Macaca mulatta*, 9-year-old male, 14 kg). All animal procedures were approved by the University of Washington Institutional Animal Care and Use Committee.

B. Electrode array and structural components

The electrode array and structural components are adapted and optimized from our previously published designs [7], [8], [14], [15].

Multi-modal artificial dura (MMAD): We previously characterized and acutely validated our large-scale semi-transparent flexible electrode array (MMAD; Ripple Neuro, Salt Lake City, UT, USA) with multiple NHPs [15], [16]. The MMAD is composed of platinum particles dispersed in a matrix within a medical grade polymer. We also previously published a method of molding the MMAD with polydimethylsiloxane (PDMS) into a top-hat shaped artificial dura for use in chronic implantations [14], similar to electrode-free designs of our previous work [7], [8] and the work of others [11]–[13]. In this work, we report the MMAD's utility for chronic cortical use in NHPs.

Chamber and cap: We custom-designed a chamber to fit onto the NHP's skull (Fig. 1a-c) and house the MMAD. The chamber was 3D printed with a titanium alloy (Ti-6Al-4V, Hybex Innovations, Anjou, QC, Canada).

In our previous work we published an MRI-based method of designing the chamber flange to fit the skull based on first-order skull curvature approximations. [8]. After updating our chamber design with a larger footprint, we discovered our previous design method was inadequate at this new scale so a new design method was needed. We built upon our MRI-based skull-extraction process [17] to develop a simple yet effective

*Research supported by R01 NS119395 (D. Griggs, A. Yazdan-Shahmorad, J. Bloch), R01 NS116464-01 (A. Yazdan-Shahmorad), University of Washington Big Data for Genomics & Neuroscience Training Grant (J. Bloch), University of Washington Mary Gates Scholarship (W. K. S. Ojemann, K. M. Coubrough), National Science Foundation Graduate Research Fellowships Program (K. Khateeb), Weill Neurohub (S. Fisher), Washington National Primate Research Center P51 OD010425 (all authors).

D. J. Griggs, J. Bloch, S. Fisher, K. Khateeb, M. Chu, and A. Yazdan-Shahmorad (corresponding author; e-mail: azadehy@uw.edu) are with University of Washington, Seattle, WA 98105 USA.

W. K. S. Ojemann was with University of Washington, Seattle and is now with University of Pennsylvania.

K. M. Coubrough was with University of Washington, Seattle and is now with the Spanish Ministry of Education.

method of custom-designing the flange with much greater detail (Fig. 1a-c). Our process capitalizes on importing a digital representation of the skull directly into modeling software for chamber design.

We designed a cap (not shown; stainless steel 304, Hybex Innovations) to close the chamber between experiments.

Recording components: We custom designed a stack-up of parts to collect electrophysiological recordings from the MMAD (Fig. 1d) similar to our previous work [14]. The stack-up included a ring (stainless steel 304, Hybex Innovations), a clamp-connector holder (Ti-6Al-4V, i.materialise, Leuven, Belgium), and clamp-connectors (Ripple Neuro), the latter being previously validated with the MMAD [15].

Stimulation components: We optimized a laser stimulation system (not shown) with minor modifications of previous work [7], [8]. Both the base and sleeve were 3D printed in-house with polylactic acid (PLA). To facilitate large-scale experimentation, we designed our light emitting diode (LED) stimulation system to provide $\sim 1 \text{ cm}^2$ of patterned illumination (Fig. 1e). The base, tube, and rod were 3D printed in-house with PLA.

C. Electronics and optics

We used a red laser (638 nm, Doric, QC, Canada) and fiberoptic cable for precise spatial stimulation. We used a simple, custom-designed miniature array ($\varnothing 15.5 \text{ mm}$, Osh Park, Portland, OR, USA) of red LEDs (634 nm, L1C1-RED1000000000, Lumileds Holding B. V., Amsterdam, Netherlands) in a 4-by-4 grid and simple, custom driving circuitry using commercially available components for large-scale, patterned stimulation (Fig. 2). Our current design offers row-by-row patterned illumination.

D. Surgical procedures

We implanted a titanium headpost (6-FHP-X2F, Crist Instrument Co., Hagerstown, MD, USA). After the animal recovered and was trained to headpost, we implanted the chamber and MMAD by performing a craniotomy and durotomy using methods similar to our previous work [8], which provided optical and electrophysiological access to the left hemisphere posterior parietal cortex (PPC; Fig. 3a-b). During the surgery, we infused optogenetic viral vector (AAV8-hSyn-Jaws-GFP, UNC Vector Core, NC, USA) at eight locations throughout the PPC (Fig. 3c) using convection-enhanced delivery (CED). Our CED methods were largely similar to our previous work [8], [18] with one key exception: past infusions were generally monitored with live MRI [8], but in this work we manually observed all

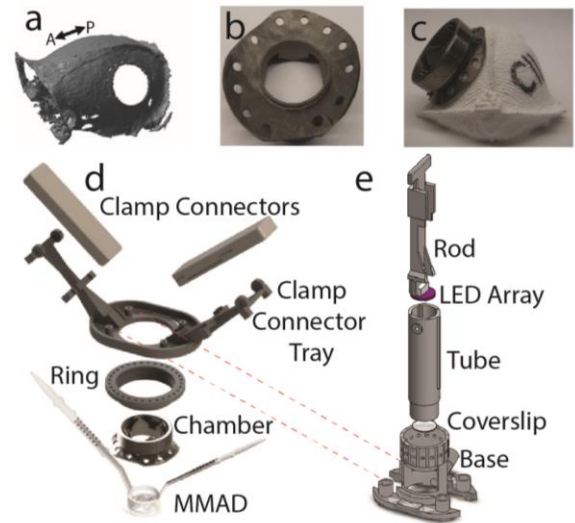


Figure 1: Cortical interface. (a) Recreation of NHP skull from MRI data with added craniotomy. (b) Skull-fitting flange of chamber. (c) Chamber fitted on a 3D printed recreation of NHP skull. (d) Stack-up for electrophysiology recording. (e) Stack-up for LED stimulation.

cannula insertions and viral infusions. During infusions we were careful to note any backflow leakage and adjust our protocol accordingly.

E. Data collection

We collected all data while the animal was awake and head-fixed. The animal watched cartoons during electrophysiology, laser stimulation, and LED stimulation. We controlled electrophysiological data collection and LED stimulation with a Grapevine Nomad (Ripple Neuro) and custom code (MATLAB, MathWorks, Natick, MA, USA), and we controlled laser stimulation with commercial software (Doric). We collected epifluorescent images of the cortex with a common digital single-lens reflex (DSLR) camera and lens in conjunction with an epifluorescent imaging system (440-460 nm excitation, 500 nm longpass emission filter, SFA-RB, Nightsea LLC, Lexington, MA, USA).

III. RESULTS

A. Optical access

We monitored optical access of the MMAD for 14 weeks after implantation and observed only minor tissue growth on the surface of the brain (Fig. 3a-b). This result is comparable to optical longevity attained by traditional, electrode-free PDMS artificial duras [8], [11]–[13].

B. Optogenetic expression

We started monitoring optogenetic expression with epifluorescent imaging two weeks after infusion and stopped six weeks after infusion. Expression was apparent during the first imaging session and increased in coverage and intensity until the fifth week after infusion, where expression plateaued at tens of mm^2 coverage (Fig. 3d). This large area of coverage is comparable with our previous work [8] and is an important proof of concept for our novel method of optogenetic CED in NHPs without live MRI guidance.

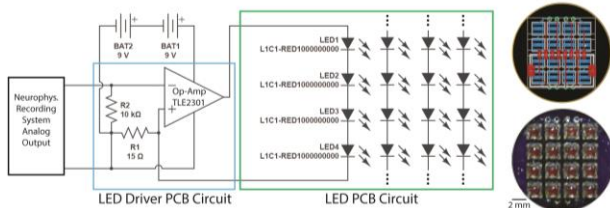


Figure 2: LED array. Circuit diagram for LED array and driving electronics (left). Each row of LEDs has its own copy of the driver circuit shown, all sharing a common power supply and occupying the same PCB (schematic, top right; image, bottom right).

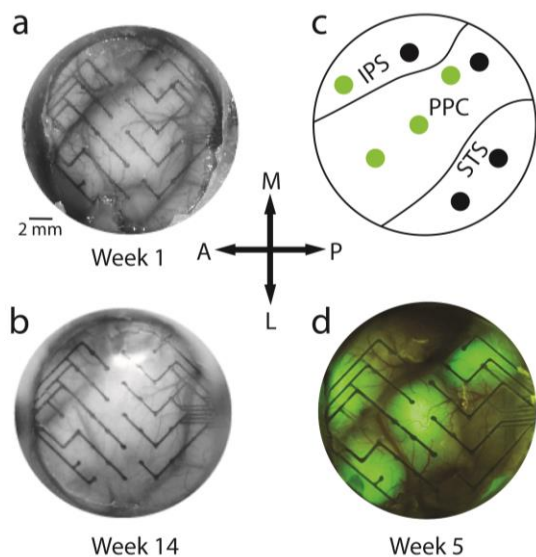


Figure 3: Optical access and optogenetic expression. Image of MMAD on the cortex one week (a) and 14 weeks (b) after implantation and infusion of optogenetic viral vector. (c) Map of optogenetic viral vector injection locations. Green circles indicate successful injections and black circles indicate unsuccessful injections. (d) Epifluorescence imaging of optogenetic expression five weeks after implantation and infusion.

C. Optogenetic modulation of neural activity

Using our laser setup eight weeks after infusion, we illuminated neural tissue with fiberoptic cable near selected electrodes and evoked spatially specific changes in our ECoG signal confirmed with various illumination parameters. Fig. 4a shows an example.

Nine weeks after illumination, we tested our LED setup by illuminating PPC ($\sim 1 \text{ cm}^2$) with the entire LED array while varying the illumination parameters (an example shown in Fig. 4b). To characterize the response, we calculated power spectral densities (PSD) of our ECoG recording from before and during stimulation (Fig. 4c). The comparison between the ratio of the PSD during and before stimulation, with that of similar data collected in saline, indicated successful neuromodulation, including depression in the 8-39 Hz range (Fig. 4d). To our knowledge, this is the largest optogenetic modulation in neuroscience to date. Further investigation is needed to elucidate the intricacies of our spectral results.

Six months after infusion, no cortical features, such as sulci or vasculature, were visible by eye due to opaque tissue growth on the surface of the brain (data not shown). At this time we repeated the LED stimulation protocol and still observed spatially broad electrophysiological depression despite the tissue growth. This result is likely due to the enhanced penetration of red light into neural tissue compared to shorter wavelengths, such as blue, which we previously found was unable to evoke neural responses under similar conditions [7]. Our finding is in agreement with past experiments testing optical penetration of tissue for the purpose of activating Jaws [19].

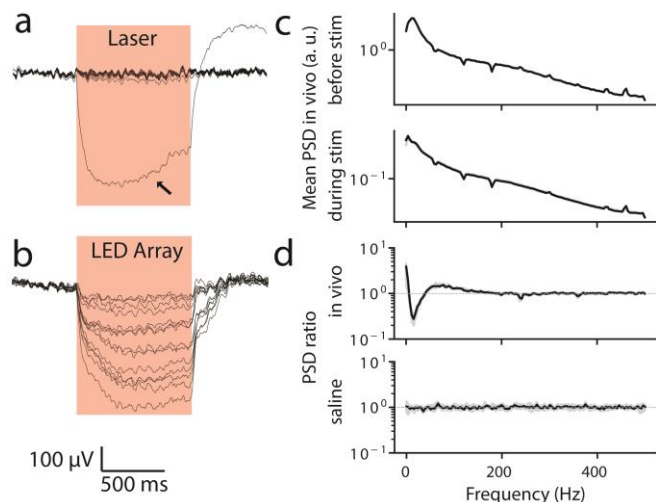


Figure 4: Neurophysiology. (a) Time-averaged wideband signals from laser light illumination (30 pulses, 900 ms per pulse at 110 mA, 27 mW optical power) *in vivo*. The stimulated channel is indicated with an arrow. Stimulation times are shown in red. (b) Time-averaged wideband signals from 30 pulses of the full LED array illumination (30 pulses, 900 ms per pulse at 700 mV, $\sim 2.4 \text{ mW/mm}^2$ optical power) *in vivo*. (c) Averaged power spectral density (PSD) before (top) and during (bottom) LED array stimulation *in vivo*. (d) Ratio of the PSD (during stim / before stim) for *in vivo* (top) and saline data (bottom). Dashed line indicates no change. Data above the dashed line indicates excitation, and below the line indicates inhibition. Shaded error bars are 95% confidence interval of median.

IV. DISCUSSION

We present simple, approachable engineering methods for attaining large-scale optogenetic and electrophysiological access to NHP cortex. All parts can be commercially purchased or made in-house with modest effort which enables the scientific community to implement large-scale optogenetic interfaces in NHPs without the need for sophisticated engineering technologies. Our novel, commercially available MMAD provides more than three months of chronic optical access to NHP cortex which is comparable to durations achieved with traditional electrode-free artificial duras [8], [11]–[13]. We attribute this success to the electrodes being printed directly into the artificial dura (creating an MMAD) as opposed to our previous two-part system [7] and our MMAD being left chronically implanted as opposed to our previous system of daily implantation and explantation of the electrode array [8]. This system equips the scientific community to pursue experiments which require or would benefit from chronic multi-modal interfaces.

Our simple LED setup provides broad, patterned illumination of the cortex which facilitates complex experiments involving multiple brain areas and complements the spatially specific experiments facilitated by our laser setup. Our LED setup is designed for easy implementation for researchers with modest electronic fabrication experience and it is compatible with our past work [7], [8]. Notably, in comparison with a recently published LED array system for NHPs [20], our LED setup provides roughly 4 times more area of stimulation. Additionally, unlike [20], our setup is compatible with both electrophysiology and cortical imaging, and our system does not require surgical intervention for LED hardware changes which drastically simplifies the process of modifying experimental design.

We demonstrated that large-scale optogenetic expression can be achieved with CED without the added experimental complexity of MRI-guidance, which makes large-scale optogenetic experiments much more accessible to the scientific community. Although MRI-free CED does not allow researchers to visualize infusion during surgery, it allows researchers to visually observe cannula penetration into the brain and the occurrence of backflow (if any). Additionally, we have developed simple bench-side modeling methods to estimate CED coverage in preparation for surgery [17]. Critically, we recently observed strong optogenetic expression six months after infusion based on electrophysiological responses evoked with low optical power (~ 2.4 mW/mm²), which suggests our animal will continue to be suitable for optogenetic experiments for additional months or years. This is in agreement with the strong, long-term (27 months with experimental termination for histological analysis) excitatory optogenetic expression we have previously achieved [8].

V. CONCLUSION

Here we present our optimized large-scale optogenetic and electrophysiological interface designed for the NHP cortex. Our work paves a path for the scientific community towards accessible long-term and large-scale optogenetic experiments in these animals that share a large degree of similarity in anatomy and physiology with humans. Our work promises to propel large-scale neuroscience research, especially in the context of connectivity and plasticity [21], [22], the development of neural disease models (e.g., [16], [23]), and the advancement of growing fields such as brain-computer interfaces and neural stimulation-based therapies.

ACKNOWLEDGMENT

We thank Mona Rahimi for her help with LED testing, Shivalika Chavan and Kelly Morrisroe for their help with animal training, and A. Graham Johnson for his help with component design. We thank the Ripple Neuro team Alex Johnson, Jose Ortega, and Jessi Michel for their help with MMAD design and production. We thank the staff of the Washington National Primate Research Center for their help with animal care.

REFERENCES

- [1] O. Yizhar, L. E. Fenno, T. J. Davidson, M. Mogri, and K. Deisseroth, "Optogenetics in neural systems," *Neuron*, vol. 71, no. 1, pp. 9–34, 2011, doi: 10.1016/j.neuron.2011.06.004.
- [2] Y. El-Shamayleh and G. D. Horwitz, "Primate optogenetics: Progress and prognosis," *Proc. Natl. Acad. Sci. U. S. A.*, vol. 116, no. 52, pp. 26195–26203, 2019, doi: 10.1073/pnas.1902284116.
- [3] A. Galvan *et al.*, "Nonhuman primate optogenetics: Recent advances and future directions," *J. Neurosci.*, vol. 37, no. 45, pp. 10894–10903, 2017, doi: 10.1523/JNEUROSCI.1839-17.2017.
- [4] A. Galvan, M. J. Caiola, and D. L. Albaugh, "Advances in optogenetic and chemogenetic methods to study brain circuits in non-human primates," *J. Neural Transm.*, vol. 125, no. 3, pp. 547–563, 2018, doi: 10.1007/s00702-017-1697-8.
- [5] S. Tremblay *et al.*, "An Open Resource for Non-human Primate Optogenetics," *Neuron*, pp. 1–16, 2020, doi: 10.1016/j.neuron.2020.09.027.
- [6] A. Yazdan-Shahmorad, D. B. Silversmith, and P. N. Sabes, "Novel techniques for large-scale manipulations of cortical networks in non-human primates," *Conf Proc IEEE Eng Med Biol Soc*, vol. 2018, pp. 5479–5482, 2018, doi: 10.1109/EMBC.2018.8513668.
- [7] A. Yazdan-Shahmorad *et al.*, "Demonstration of a setup for chronic optogenetic stimulation and recording across cortical areas in non-human primates," *SPIE BiOS*, vol. 9305, no. March 2015, p. 93052K, 2015, doi: 10.1117/12.2080405.
- [8] A. Yazdan-Shahmorad *et al.*, "A Large-Scale Interface for Optogenetic Stimulation and Recording in Nonhuman Primates," *Neuron*, vol. 89, no. 5, pp. 927–939, 2016, doi: 10.1016/j.neuron.2016.01.013.
- [9] D. J. Griggs, T. Belloir, and A. Yazdan-Shahmorad, "Large-scale neural interfaces for optogenetic actuators and sensors in non-human primates," *SPIE BiOS*, vol. 1166305, no. March, p. 17, 2021, doi: 10.1117/12.2579431.
- [10] P. Ledochowitsch *et al.*, "Strategies for optical control and simultaneous electrical readout of extended cortical circuits," *J. Neurosci Methods*, vol. 256, pp. 220–231, 2015, doi: 10.1016/j.jneumeth.2015.07.028.
- [11] A. Arieli, A. Grinvald, and H. Slovin, "Dural substitute for long-term imaging of cortical activity in behaving monkeys and its clinical implications," *J. Neurosci. Methods*, vol. 114, no. 2, pp. 119–133, 2002, doi: 10.1016/S0165-0270(01)00507-6.
- [12] L. M. Chen, R. M. Friedman, and A. W. Roe, "Optical imaging of SI topography in anesthetized and awake squirrel monkeys," *J. Neurosci.*, vol. 25, no. 33, pp. 7648–7659, 2005, doi: 10.1523/JNEUROSCI.1990-05.2005.
- [13] O. Ruiz *et al.*, "Optogenetics through windows on the brain in the nonhuman primate," *J. Neurophysiol.*, vol. 110, no. 6, pp. 1455–1467, 2013, doi: 10.1152/jn.00153.2013.
- [14] D. J. Griggs, K. Khateeb, S. Philips, J. W. Chan, W. Ojemann, and A. Yazdan-Shahmorad, "Optimized large-scale optogenetic interface for non-human primates," p. 3, 2019, doi: 10.1117/12.2511317.
- [15] D. J. Griggs, K. Khateeb, J. Zhou, T. Liu, R. Wang, and A. Yazdan-Shahmorad, "Multi-modal artificial dura for simultaneous large-scale optical access and large-scale electrophysiology in non-human primate cortex," *J. Neural Eng. Spec. Issue "Neuroelectronic Interfaces"*, vol. 18, no. 5, p. 2021.02.03.429596, 2021, doi: 10.1101/2021.02.03.429596.
- [16] K. Khateeb *et al.*, "A versatile toolbox for studying cortical physiology in primates," *Cell Reports Methods*, p. 100183, 2022, doi: 10.1016/j.crmeth.2022.100183.
- [17] W. K. S. Ojemann *et al.*, "A mri-based toolbox for neurosurgical planning in nonhuman primates," *J. Vis. Exp.*, vol. 2020, no. 161, pp. 1–16, 2020, doi: 10.3791/61098.
- [18] K. Khateeb, D. J. Griggs, P. N. Sabes, and A. Yazdan-Shahmorad, "Convection Enhanced Delivery of Optogenetic Adeno-associated Viral Vector to the Cortex of Rhesus Macaque Under Guidance of Online MRI Images," *J Vis Exp*, no. 147, pp. 1–8, 2019, doi: 10.3791/59232.
- [19] L. Acker, E. N. Pino, E. S. Boyden, and R. Desimone, "FEF inactivation with improved optogenetic methods," *Proc Natl Acad Sci U S A*, vol. 113, no. 46, pp. E7297–E7306, 2016, doi: 10.1073/pnas.1610784113.
- [20] R. Rajalingham, M. Sorenson, R. Azadi, S. Bohn, J. J. DiCarlo, and A. Afraz, "Chronically implantable LED arrays for behavioral optogenetics in primates," *Nat. Methods*, vol. 18, no. 9, pp. 1112–1116, 2021, doi: 10.1038/s41592-021-01238-9.
- [21] A. Yazdan-Shahmorad, D. B. Silversmith, V. Kharazia, and P. N. Sabes, "Targeted cortical reorganization using optogenetics in non-human primates," *Elife*, vol. 7, pp. 1–21, 2018, doi: 10.7554/eLife.31034.
- [22] J. A. Bloch, K. Khateeb, D. B. Silversmith, J. E. O'Doherty, P. N. Sabes, and A. Yazdan-Shahmorad, "Cortical Stimulation Induces Network-Wide Coherence Change in Non-Human Primate Somatosensory Cortex*," *Proc. Annu. Int. Conf. IEEE Eng. Med. Biol. Soc. EMBS*, pp. 6446–6449, 2019, doi: 10.1109/EMBC.2019.8856633.
- [23] K. Khateeb *et al.*, "A Practical Method for Creating Targeted Focal Ischemic Stroke in the Cortex of Nonhuman Primates()," *Conf Proc IEEE Eng Med Biol Soc*, vol. 2019, pp. 3515–3518, 2019, doi: 10.1109/EMBC.2019.8857741.